

**Spatial interpolation of daily rainfall**

S. Ly et al.

This discussion paper is/has been under review for the journal Hydrology and Earth System Sciences (HESS). Please refer to the corresponding final paper in HESS if available.

# Spatial interpolation of daily rainfall at catchment scale: a case study of the Ourthe and Ambleve catchments, Belgium

S. Ly<sup>1</sup>, C. Charles<sup>2</sup>, and A. Degré<sup>1</sup>

<sup>1</sup>University of Liege, Gembloux Agro-Bio Tech, Unit of Hydrology and Agricultural Hydraulic, Gembloux, Belgium

<sup>2</sup>University of Liege, Gembloux Agro-Bio Tech, Unit of Applied Statistics, Computer Science and Mathematics, Gembloux, Belgium

Received: 16 September 2010 – Accepted: 20 September 2010  
– Published: 27 September 2010

Correspondence to: S. Ly (sarann.ly@doct.ulg.ac.be)

Published by Copernicus Publications on behalf of the European Geosciences Union.

Title Page	
Abstract	Introduction
Conclusions	References
Tables	Figures
◀	▶
◀	▶
Back	Close
Full Screen / Esc	
Printer-friendly Version	
Interactive Discussion	



## Abstract

Spatial interpolation of precipitation data is of great importance for hydrological modelling. Geostatistical methods (krigings) are widely used in spatial interpolation from point measurement to continuous surfaces. However, the majority of existing geostatistical algorithms are available only for single-moment data. The first step in kriging computation is the semi-variogram modelling which usually uses only one variogram model for all-moment data. The objective of this paper was to develop different algorithms of spatial interpolation for daily rainfall on 1 km<sup>2</sup> regular grids in the catchment area and to compare the results of geostatistical and deterministic approaches. In this study, we used daily rainfall data from 70 raingages in the hilly landscape of the Ourthe and Ambleve catchments in Belgium (2908 km<sup>2</sup>). This area lies between 35 and 693 m in elevation and consists of river networks, which are tributaries of the Meuse River. For geostatistical algorithms, Cressie's Approximate Weighted Least Squares method was used to fit seven semi-variogram models (logarithmic, power, exponential, Gaussian, rational quadratic, spherical and penta-spherical) to daily sample semi-variogram on a daily basis. Seven selected raingages were used to compare the interpolation performance of these algorithms applied to many degenerated-raingage cases. Spatial interpolation with the geostatistical and Inverse Distance Weighting (IDW) algorithms outperformed considerably interpolation with the Thiessen polygon that is commonly used in various hydrological models. Kriging with an External Drift (KED) and Ordinary Cokriging (OCK) presented the highest Root Mean Square Error (RMSE) between the geostatistical and IDW methods. Ordinary Kriging (ORK) and IDW were considered to be the best methods, as they provided smallest RMSE value for nearly all cases.

## 1 Introduction

Basin management, including hydrological and water quality applications, requires data on the very important precipitation parameter. These data are always collected using

# HESSD

7, 7383–7416, 2010

## Spatial interpolation of daily rainfall

S. Ly et al.

Title Page

Abstract

Introduction

Conclusions

References

Tables

Figures

◀

▶

◀

▶

Back

Close

Full Screen / Esc

Printer-friendly Version

Interactive Discussion



**Spatial interpolation  
of daily rainfall**

S. Ly et al.

Title Page

Abstract

Introduction

Conclusions

References

Tables

Figures

◀

▶

◀

▶

Back

Close

Full Screen / Esc

Printer-friendly Version

Interactive Discussion



raingages, and hence they are point data. However, use of a single raingage as rain-  
fall input carries great uncertainties regarding runoff estimation (Faurès et al., 1995;  
Chaubey et al., 1999). This presents a great problem for the prediction of discharge,  
groundwater level and soil moisture, especially if the raingage is situated outside the  
catchment (Schuurmans and Bierkens, 2007). As a result, some applications such  
as rainfall erosivity mapping (Aronica and Ferro, 1997; Goovaerts, 1999; Hoyos et al.,  
2005; Nyssen et al., 2005; Angulo-Martinez et al., 2009a,b) and hydrological modelling  
(Syed et al., 2003; Kobold and Sušelj, 2005; Gabellani et al., 2007; Cole and Moore,  
2008; Collischonn et al., 2008; Ruelland et al., 2008; Moulin et al., 2009) require rainfall  
data that are spatially continuous. The quality of such result is thus determined by the  
quality of the continuous spatial rainfall (Singh, 1997; Andréassian et al., 2001; Kobold  
and Sušelj, 2005; Leander et al., 2008; Moulin et al., 2009).

The generation of continuous surfaces starting from irregularly distributed data is  
a task for many disciplines. It can be performed by a variety of methods but the dif-  
ficulty lies in choosing the one that best reproduces the actual surface (Caruso and  
Quarta, 1998). Indirect estimates of continuous surface based on the measurement of  
related ancillary variables have been provided since the late 1960s by ground-based  
meteorological RADARs and by remote sensing devices carried on satellite platforms.  
The significance and reliability of such indirect methods for hydrological purposes have  
still to be determined. The methods must be calibrated and validated using historical  
data (Lanza et al., 2001). However for direct ground-based measurement, spatial inter-  
polation techniques can be broadly classified into two main groups: deterministic and  
geostatistical.

The first group, deterministic methods, considers that the estimates of regional value  
take the form of the weighted mean of observed regional values. The simplest method,  
the Thiessen polygon, assumes that the amount of rainfall at any station can be applied  
halfway to the next station in any direction (Chow, 1964). Another of the most frequently  
used deterministic methods in spatial interpolation is the Inverse Distance Weighting  
(IDW) method. The latter is relatively fast, easy to compute, and straightforward to

interpret. Its general idea is based on the assumption that the attribute value of an un-sampled point is the weighted average of known values within the neighbourhood, the weights being inversely related to the distances between the prediction and the sampled locations (Teegavarupu and Chandramouli, 2005; Lu and Wong, 2008).

5 The second group of spatial interpolation techniques, geostatistical methods, constitutes a discipline involving mathematics and earth sciences. The work of Krige, a South African mine engineer, is a precursor of geostatistics. Nevertheless, the term “kriging” and the formalism of this method are due to Matheron (1971).

10 Several authors have compared various deterministic and geostatistical approaches to one another in spatial rainfall interpolation. For example, Dirks et al. (1998) compared Inverse Distance Weighting, the Thiessen polygon and kriging in interpolating rainfall data from a network of thirteen raingages on Norfolk Island. Nalder and Wein (1998) used cross validation to evaluate four forms of kriging and three simple alternatives for spatial interpolation of climatic data in the Canadian boreal forest. Buytaert et al. (2006) studied the variability of spatial and temporal rainfall in the South Ecuadorian Andes using the Thiessen polygon and kriging. Basistha et al. (2008) analysed the spatial distribution of rainfall in the Indian Himalayas using both deterministic and geostatistical methods. Goovaerts (2000) and Lloyd (2005) used elevation as secondary data to incorporate into multivariate geostatistics for monthly and annual rainfall and compared these results with those of deterministic methods. Overall, they found that the geostatistical and IDW methods provided better result than the other deterministic techniques.

25 Hydrological models have traditionally used rainfall data interpolated from the Thiessen polygon. Most of applications consider only monthly or annual time steps for spatial interpolation of precipitation (Hevesi et al., 1992; Goovaerts, 2000; Boer et al., 2001; Todini, 2001; Marquínez et al., 2003; Vicente-Serrano et al., 2003; Lloyd, 2005) but some others used hourly time steps for large-scale extreme rainfall events (Haberlandt, 2007). They usually apply the same theoretical variogram model for each time step when they interpolate rainfall using the geostatistical methods. However,

## Spatial interpolation of daily rainfall

S. Ly et al.

Title Page

Abstract

Introduction

Conclusions

References

Tables

Figures

◀

▶

◀

▶

Back

Close

Full Screen / Esc

Printer-friendly Version

Interactive Discussion



a daily time step is optimal for an understanding of the soil-plant-water relationship and long-term catchment management simulation.

The objective of this study is to obtain the best interpolation method to produce daily rainfall data for hydrological models. We develop algorithms for spatial interpolation of daily rainfall data on 1 km<sup>2</sup> regular grids at the catchment scale, taking into consideration the automatic choice of a daily based theoretical variogram model for geostatistical methods. The algorithm will be applied to different cases degenerating into different numbers of raingages inside and surrounding the catchment. This approach addresses key questions: which method gives the best results? With the raingage in which position? Can secondary data improve the results? The results of the interpolated rainfall using geostatistical methods were compared to the reference of deterministic methods (Thiessen polygon and Inverse Distance Weighting).

## 2 Materials and methods

In this paper, geostatistical algorithms (ordinary kriging, universal kriging, kriging with an external drift and ordinary cokriging), deterministic algorithms (Thiessen polygon and inverse distance weighting) were developed using Fortran 90 to produce the daily rainfall of each grid from 1976 to 2005. The performance of these methods was then evaluated.

### 2.1 Interpolation procedures

The interpolation methods used in this paper will be briefly introduced. A detailed presentation of geostatistical theories can be found in Cressie (1991), Goovaerts (1997), Chilès and Delfiner (1999), and Webster and Oliver (2007).

Spatial interpolation is generally carried out by estimating a regionalized value at un-sampled points from a weight of observed regionalized values. In this study, un-sampled points refer to the centres of 1-km<sup>2</sup>-regular grids in the catchment area. The

## Spatial interpolation of daily rainfall

S. Ly et al.

Title Page

Abstract

Introduction

Conclusions

References

Tables

Figures

◀

▶

◀

▶

Back

Close

Full Screen / Esc

Printer-friendly Version

Interactive Discussion



general formula for spatial interpolation is as follows:

$$Z_g = \sum_{i=1}^{ns} \lambda_i Z_{s_i} \quad (1)$$

where  $Z_g$  is the interpolated value at point  $g$ ,  $Z_{s_i}$  is the observed value at point  $i$ ,  $ns$  is the total number of observed points (raingages) and  $\lambda = (\lambda_i)$  is the weight contributing to the interpolation.

The problem lies in calculating the weights  $\lambda$ , which will be used in the interpolation. The different methods for computing the weights will be presented in the following sections.

### 2.1.1 Deterministic methods

#### Thiessen polygon (THI)

For the Thiessen polygon, the catchment area is divided into polygons so that each polygon contains a single point of sampling (recorded raingages). Each interpolated point (centre of each grid) takes the value of the closest sampled point. The advantage of this method is its simplicity. However, the disadvantages of this method are obvious – the estimation is based on only one measurement and the information on neighbouring points is ignored. Moreover, there are sudden jumps of discontinuity in the passage from one polygon to another.

#### Inverse Distance Weighting (IDW)

Inverse Distance Weighting (IDW) estimates values at un-sampled points by the weighted average of observed data at surrounding points. So, this can be defined as a distance reverse function of each point from neighbouring points. That means by using a linear combination of values at a known sampled point, values at un-sampled points can be calculated. IDW relies on the theory that the unknown value of a point is

## Spatial interpolation of daily rainfall

S. Ly et al.

Title Page

Abstract

Introduction

Conclusions

References

Tables

Figures

◀

▶

◀

▶

Back

Close

Full Screen / Esc

Printer-friendly Version

Interactive Discussion



influenced by closer points than by points further away. The weight can be computed by:

$$\lambda_i = \frac{\frac{1}{|D_i|^d}}{\sum_{i=1}^{ns} \frac{1}{|D_i|^d}}, \quad d > 0 \quad (2)$$

where  $D_i$  is the distance between sampled and un-sampled points. The  $d$  parameter is specified as a geometric form for the weight while other specifications are possible. This specification implies that if the power  $d$  is larger than 1, the so-called distance-decay effect will be more than proportional to an increase in distance, and vice versa. Thus, small power  $d$  tends to give estimated values as averages of  $Zs_i$  in the neighbourhood, while large power  $d$  tends to give larger weights to the nearest points and increasingly down-weights points further away (Lu and Wong, 2008). Using a power value of 2 for daily and monthly time steps, 3 for hourly and 1 for yearly would appear to minimize the interpolation errors (Dirks et al., 1998). Furthermore, this power  $d$  is usually set to 2, following Goovaert (2000) and Lloyd (2005) and hence inverse square distances are used in the estimation. Consequently, a power value of 2 was adopted for IDW in this study.

### 2.1.2 Geostatistical methods

Geostatistical methods use the semi-variograms as a core tool to characterize the spatial dependence in the property of interest. Figure 1 shows a simplified flowchart of kriging computations procedures carried out in this study.

## Spatial interpolation of daily rainfall

S. Ly et al.

Title Page

Abstract

Introduction

Conclusions

References

Tables

Figures

◀

▶

◀

▶

Back

Close

Full Screen / Esc

Printer-friendly Version

Interactive Discussion



## Variogram modelling

First of all, the experimental semi-variogram was calculated as a half the squares difference between paired values to distance by which they were separated:

$$\hat{\gamma}(h) = \frac{1}{2N(h)} \sum_{i=1}^{N(h)} (Zs_i - Z(s_i + h))^2 \quad (3)$$

5 where  $N(h)$  is the number of pairs of data locations a vector  $h$  apart. The spatial variability was assumed here to be an isotropic spatial pattern due to the lack of number of points data, and hence identical variability in all directions.

10 In practice, the average squared distance was obtained for all pairs separated by a range of distances and these average squares differences were plotted against the average separation distance. A theoretical model might then be fitted to the experimental semi-variogram and the coefficient of this model could be used for kriging. Most previous studies have used only one theoretical model for each time step, and these were mostly in monthly or yearly steps (Hevesi et al., 1992; Goovaerts, 2000; Boer et al., 2001; Todini, 2001; Marquínez et al., 2003; Lloyd, 2005). However, this paper focuses on daily data over 30 years. On a daily basis, rainfall has different spatial variability. In this study, we dealt with the fitting of the semi-variogram for every day of our 30-year period. In order to do this, we used seven existing theoretical models, as presented below:

– De Wijs (logarithmic) model:

$$\gamma(h; \theta) = \begin{cases} 0, & h = 0, \\ \theta_0 + \theta_1 \ln \|h\|, & h \neq 0, \end{cases} \quad (4)$$

20 for  $\theta_0 \geq 0$  and  $\theta_1 \geq 0$ .

Title Page

Abstract

Introduction

Conclusions

References

Tables

Figures

◀

▶

◀

▶

Back

Close

Full Screen / Esc

Printer-friendly Version

Interactive Discussion



– Power model:

$$\gamma(h; \theta) = \begin{cases} 0, & h = 0, \\ \theta_0 + \theta_1 \|h\|^{\theta_2}, & h \neq 0, \end{cases} \quad (5)$$

for  $\theta_0 \geq 0, \theta_1 \geq 0$  and  $0 \leq \theta_2 < 2$ .

– Exponential model:

$$\gamma(h; \theta) = \begin{cases} 0, & h = 0, \\ \theta_0 + \theta_1 [1 - \exp(-3\|h\|/\theta_2)], & h \neq 0, \end{cases} \quad (6)$$

for  $\theta_0 \geq 0, \theta_1 \geq 0$  and  $\theta_2 \geq 0$ .

5 – Gaussian model:

$$\gamma(h; \theta) = \begin{cases} 0, & h = 0, \\ \theta_0 + \theta_1 \left\{ 1 - \exp \left[ -3 \left( \|h\| / \theta_2 \right)^2 \right] \right\}, & h \neq 0, \end{cases} \quad (7)$$

for  $\theta_0 \geq 0, \theta_1 \geq 0$  and  $\theta_2 \geq 0$ .

– Rational quadratic model:

$$\gamma(h; \theta) = \begin{cases} 0, & h = 0, \\ \theta_0 + \theta_1 \frac{19 \left( \|h\| / \theta_2 \right)^2}{1 + 19 \left( \|h\| / \theta_2 \right)^2}, & h \neq 0, \end{cases} \quad (8)$$

for  $\theta_0 \geq 0, \theta_1 \geq 0$  and  $\theta_2 \geq 0$ .

## Spatial interpolation of daily rainfall

S. Ly et al.

Title Page

Abstract

Introduction

Conclusions

References

Tables

Figures

◀

▶

◀

▶

Back

Close

Full Screen / Esc

Printer-friendly Version

Interactive Discussion



– Spherical model:

$$\gamma(h; \theta) = \begin{cases} 0, & h = 0, \\ \theta_0 + \theta_1 \left( \frac{3\|h\|}{2\theta_2} - \frac{1}{2} \left( \frac{\|h\|}{\theta_2} \right)^3 \right), & 0 < \|h\| \leq \theta_2, \\ \theta_0 + \theta_1, & h \neq 0, \end{cases} \quad (9)$$

for  $\theta_0 \geq 0, \theta_1 \geq 0$  and  $\theta_2 \geq 0$ .

– Penta-spherical model

$$\gamma(h; \theta) = \begin{cases} 0, & h = 0, \\ \theta_0 + \theta_1 \left( \frac{15\|h\|}{8\theta_2} - \frac{5}{4} \left( \frac{\|h\|}{\theta_2} \right)^3 + \frac{3}{8} \left( \frac{\|h\|}{\theta_2} \right)^5 \right), & 0 < \|h\| \leq \theta_2, \\ \theta_0 + \theta_1, & h \neq 0, \end{cases} \quad (10)$$

for  $\theta_0 \geq 0, \theta_1 \geq 0$  and  $\theta_2 \geq 0$ .

5 Each of these models was combined with a nugget effect. The most common methods of fitting semi-variogram models to experimental semi-variogram models are performed by eye. However, this is not an appropriate approach because it depends on the expertise and the information in the field. Moreover, this procedure was not feasible for daily data of 30 years, hence instead an automatic procedure was necessary. Cressie  
 10 (1985) proposed weighted least squares, used in this study, as a reasonable compromise between the efficiency of generalized least squares and the simplicity of ordinary least squares for fitting a semi-variogram model to an experimental semi-variogram. He introduced an approximation to the weighted least squares criterion, which reduced the estimation problem to iteratively reweighted least squares:

$$15 \quad C(h; \theta) = \sum_{i=1}^K |N(h_i)| \left( \frac{\hat{\gamma}(h_i)}{\gamma(h_i; \theta)} - 1 \right)^2 \quad (11)$$

where  $h_1, h_2, \dots, h_k$  are equally spaced lags at which the semi-variogram is estimated. In this study, the coefficients of a model for kriging were chosen when the coefficient

Title Page

Abstract

Introduction

Conclusions

References

Tables

Figures

◀

▶

◀

▶

Back

Close

Full Screen / Esc

Printer-friendly Version

Interactive Discussion



## Spatial interpolation of daily rainfall

S. Ly et al.

Title Page

Abstract

Introduction

Conclusions

References

Tables

Figures

◀

▶

◀

▶

Back

Close

Full Screen / Esc

Printer-friendly Version

Interactive Discussion



$C$  was least among the iteration processes. Moreover, a model was chosen for each day by considering the model which provided the smallest  $C$  among the seven models. Figure 2 shows an example of fitting seven variogram models to the sample semi-variogram of rainfall on 7 August 1991. The rational quadratic model was chosen for this day. However, kriging can lead to negative estimates. Thus, the variogram model was changed to another one until the kriging estimates were all positives (Fig. 1).

The coefficients of the chosen model were then used to determine the weight through equation systems of different types of kriging: Ordinary Kriging (ORK), Universal Kriging (UNK), and Kriging with an External Drift (KED).

### 10 Ordinary Kriging (ORK)

The weights are obtained such that the estimation is unbiased and the variance is minimized. The ORK system of  $(ns+1)$  equations, is as follow:

$$\begin{cases} \sum_{i=1}^{ns} \lambda_i \gamma_{ij} - \mu = \gamma_{i0} & \text{for } j = 1, \dots, ns \\ \sum_{i=1}^{ns} \lambda_i = 1 \end{cases} \quad (12)$$

Where  $\gamma_{ij}$  represents the semi-variances of  $Z$ s between locations  $i$  and  $j$ , and  $\mu$  is the Lagrange parameter.

This system can be shown in matrix form to facilitate the resolution:

$$\mathbf{\Gamma} \times \boldsymbol{\lambda} = \mathbf{G} \Rightarrow \boldsymbol{\lambda} = \mathbf{\Gamma}^{-1} \times \mathbf{G} \quad (13)$$

The weights  $\lambda_i$ , obtained through this system are inserted into Eq. (1) to make the prediction. The unbiased estimate is assured by the constraint of the sum of the weight to 1, which requires the definition of the Lagrange parameter.

## Universal Kriging (UNK)

This assumes that spatial variation in estimated values has a structural component in addition to the spatial correlation between known points (Basista et al., 2008). Typically, UNK incorporates a trend surface equation in the kriging process. This can be either a first order polynomial or it can be a quadratic surface defined by a second order polynomial. The prediction is computed when the weights are such that the prediction is unbiased and the variance is minimized. The same process as in ORK is followed. The system of  $(ns+L+1)$  can be written as:

$$\begin{cases} \sum_{i=1}^{ns} \lambda_i \gamma_{ij} + \sum_{l=1}^L \mu_l f_i^l = \gamma_{i0} & \text{for } i = 1, \dots, ns \\ \sum_{i=1}^{ns} \lambda_i f_i^l = f_0^l & \text{for } l = 0, \dots, L \end{cases} \quad (14)$$

where  $\gamma_{ij}$  represents the semi-variances of  $Z$ s between locations  $i$  and  $j$ , and  $\mu_l$  are the Lagrange parameters and  $f$  is the mean which is a function of spatial coordinates. This study dealt with linear trend, hence  $L=2$ ,  $f_i^0=1$ ,  $f_i^1=x_i$ ,  $f_i^2=y_i$  ( $x$  and  $y$  are the abscise and ordinate of the points). When  $L=0$ ,  $\sum_{i=1}^{ns} \lambda_i=1$  which is the constraint of unbiased. The system can be also written in matrix form (Eq. 13) and the weights  $\lambda_i$  can be computed to make the prediction.

## Kriging with an External Drift (KED)

We made the hypothesis that the variable of interest presents a structure of ensemble modelled by a secondary variable. The spatial behaviour of the secondary variable is similar to an indicator of general trend, the so-called external drift, representative of a representation of predictions, regarding the considered geographical domain. This study dealt with the trend model of the combined function of spatial coordinates and elevation as the secondary variable simultaneously.

Title Page

Abstract

Introduction

Conclusions

References

Tables

Figures

◀

▶

◀

▶

Back

Close

Full Screen / Esc

Printer-friendly Version

Interactive Discussion



## Ordinary Cokriging (OCK)

The last of the geostatistical methods dealt with in this study is Ordinary Cokriging (OCK), which is another approach to incorporating secondary information in order to improve the spatial interpolation. Goovaerts (2000) stated that using multiple secondary variables can lead to unstable cokriging systems. Thus, only elevation ( $Y_s$ ) was considered in this paper. The cokriging estimate is:

$$Zg = \sum_{i=1}^{ns} \lambda_i Zs_i + \sum_{i=1}^{ns} \alpha_i Ys_i \quad (15)$$

where all secondary variables are obtained at the same points of variable of interest. As with ORK, the objective is to minimize the variance under the constraint of un-bias, which gives a very complex system of  $(ns+ns+2)$  equations:

$$\begin{cases} \sum_{i=1}^{ns} \lambda_i \gamma(Z_i, Z_j) + \sum_{i=1}^{ns} \alpha_i \gamma(Z_i, Y_j) + \mu_Z = \gamma(Z_0, Z_j) & \text{for } j = 1, \dots, ns \\ \sum_{i=1}^{ns} \lambda_i \gamma(Y_i, Z_j) + \sum_{i=1}^{ns} \alpha_i \gamma(Y_i, Y_j) + \mu_Y = \gamma(Z_0, Y_j) & \text{for } j = 1, \dots, ns \\ \sum_{i=1}^{ns} \lambda_i = 1 \\ \sum_{i=1}^{ns} \alpha_i = 0 \end{cases} \quad (16)$$

The system can also be written in the matrix form. There are two Lagrange parameters to take into account for the constraints on the weight of primary and secondary data. The input information  $(\gamma(Z_i, Z_j), \gamma(Y_i, Y_j), \gamma(Z_i, Y_j))$  represents the values of direct semi-variograms of primary and secondary variables and cross semi-variograms of primary

Title Page

Abstract

Introduction

Conclusions

References

Tables

Figures

◀

▶

◀

▶

Back

Close

Full Screen / Esc

Printer-friendly Version

Interactive Discussion



and secondary variables, respectively for spaced distances. The experimental cross-semi-variograms were computed as:

$$\hat{\gamma}_{ZY}(h) = \frac{1}{2N(h)} \sum_{i=1}^{N(h)} [Zs_i - Z(s_i + h)][Ys_i - Y(s_i + h)] \quad (17)$$

Modelling the co-regionalization between two variables  $Z$  and  $Y$  involves choosing and fitting theoretical models to the two direct semi-variograms  $\gamma(Z_i, Z_j)$  and  $\gamma(Y_i, Y_j)$  plus the cross semi-variogram  $\gamma(Z_i, Y_j)$ . The difficulty lies in the fact that the three models can not be built independently from one another. The easiest approach consists of modelling the three semi-variograms as linear combinations of the same set of basic semi-variogram models (Goovaerts, 1998).

The coefficients of the fitted models are used to determine the weight through the equation systems of Ordinary Cokriging (Eq. 16).

## 2.2 Study area, data and case study

In this study, we used daily rainfall data of 30 years (1976–2005) from 70 raingages within and surrounding the hilly landscape of the Ourthe and Ambleve catchments (2908 km<sup>2</sup>). These catchments were divided into regular grids of 1 km<sup>2</sup>. The catchment area lies between 35 and 693 m in elevation, and is located in the Ardennes hill range in the south-eastern part of Belgium, called the Walloon region (Fig. 3). The Ourthe River is an important tributary of the Meuse River. Since the higher Condroz region acts as a natural boundary, the Ourthe flows in a northerly direction. Several smaller tributaries, such as the Vesdre and the Ambleve, join the Ourthe River along its way towards Liege, where it eventually joins the river Meuse.

The precipitation data were provided by the Royal Meteorological Institute of Belgium. The elevation data used for this study are extracted from the Digital Elevation Model (DEM) provided by the ERRUISSOL project (Demarcin et al., 2009).

In this study, the interpolation procedures were applied to different case studies,

## Spatial interpolation of daily rainfall

S. Ly et al.

Title Page

Abstract

Introduction

Conclusions

References

Tables

Figures

◀

▶

◀

▶

Back

Close

Full Screen / Esc

Printer-friendly Version

Interactive Discussion



which consisted of degenerating into 70 (all available raingages), 60, 50, 40, 30, 20, 8 and 4 raingages.

Over the 30 years (1976–2005), there were a total of 10 063 rain days, on which the Pearson's coefficient could be computed (Fig. 4). Of these 10 063 rain days, 2087 rain days (20.74%) had a Pearson's correlation coefficient higher than 0.5 and 181 rain days (1.8%) had a Pearson's correlation coefficient lower than  $-0.5$ . In this study, a day was designated a "no-rain day" if rainfall for that day was equal to zero for all raingages of available data in the area, otherwise, the day was designated as a "rain day".

### 2.3 Evaluation criteria for interpolators

The evaluation of such a comparison of different interpolators was usually made by cross validation which involves temporarily discarding data from the sample data set; the value at the same location is then estimated using the remaining samples (Isaaks and Srivastava, 1989). Most of authors cited in this paper always use a cross validation technique with monthly or annual time steps. The sample size from the cross validation is the number of sample data (number of existing raingages). Nevertheless, it would be time consuming to use cross validation for the daily time steps of 30-year precipitation. Therefore, seven raingages in the study area were randomly selected to be used for validation, in view of the fact that the existing observed daily rainfall series of these seven raingages provided a large enough sample size. These seven raingages are FLAMIERGES (elevation 496.88), FRAITURE (elevation 235.54), LA GLEIZE (elevation 333.95), TAILLES (elevation 608.67), ROBERTVILLE (elevation 514.82), EREZEE (elevation 320.87) and SINSIN (elevation 236.1) (Fig. 3). These raingages were not included when we used 60, 50, 40, 30, 20, 8 and 4 raingages for interpolation. When using 70 raingages, one of seven raingages was temporarily removed from the 70 sample data set for each computation; the value at the same location was then estimated using the 69 remaining samples. The interpolated rainfalls were then compared to observed time series of daily rainfall at these seven raingages.

Root Mean Square Error (RMSE) has been used as a criteria of comparison in many

## Spatial interpolation of daily rainfall

S. Ly et al.

Title Page

Abstract

Introduction

Conclusions

References

Tables

Figures

◀

▶

◀

▶

Back

Close

Full Screen / Esc

Printer-friendly Version

Interactive Discussion



studies related to spatial interpolation of rainfall such as high-resolution studies of rainfall on Norfolk Island (Dirks et al., 1998), assessing the effect of integrating elevation data into the estimation of monthly precipitation in Great Britain (Lloyd, 2005), comparison of interpolation methods for mapping climatic and bioclimatic variables at regional scale in Mountain Appennines chain (Attore et al., 2007), and spatial distribution of rainfall in the Indian Himalayas (Basistha et al., 2008).

$$\text{RMSE} = \sqrt{\frac{1}{n} \sum_{i=1}^n (Zs_i^* - Zs_i)^2} \quad (18)$$

$Zs_i^*$ : observed value at the raingage;  $Zs_i$ : interpolated value at the raingage;  $n$ : sample size (total number of days).

The most accurate algorithm has an RMSE value closest to zero. Although all geostatistical methods provide an estimate of the error variance, but this value has not been retained as a performance criterion because it is not adequate to delimit the reliability of kriging estimate (Goovaert, 2000).

### 3 Results

#### 3.1 Spatial distribution of rainfall

The most straightforward method used was the Thiessen polygon (THI), whereby the value of the closest observation was simply assigned to each grid. The Thiessen polygon map showed the characteristics of the polygonal zones of influence around each raingages (Fig. 5). This method obviously provided an unrealistic discontinuous rain field at the border of each polygon, and did not show the true spatial variation of rainfall. The annual mean rainfall varied from 840 mm at the lowest elevation to 1421 mm at the highest elevation with a mean over the area of 1035 mm.

For the Inverse Distance Weighting (IDW) map, the closest measured values had the most influence. IDW used a simple algorithm based on distance. In this study, we used

## Spatial interpolation of daily rainfall

S. Ly et al.

Title Page

Abstract

Introduction

Conclusions

References

Tables

Figures

◀

▶

◀

▶

Back

Close

Full Screen / Esc

Printer-friendly Version

Interactive Discussion



inverse square distances to obtain the values at all grids in the catchment area. The map showed a distribution in more or less individual areas. Within these areas, there was usually a duck-egg shape corresponding to a high or low rainfall value (Fig. 5). The annual mean rainfall varied from 878 mm at the lowest elevation to 1330 mm at the highest elevation with a mean value over area of 1045 mm.

Instead of distance, kriging formed weights from surrounding measured values to predict values at each grid. However, the kriging weights for the surrounding measured points were more sophisticated than those produced by IDW. The kriging weights came from a semi-variogram that was developed by looking at the spatial structure of the data. The predictions of each grid were made based on the semi-variogram and the spatial arrangement of measured values that were nearby. The map generated by Ordinary Kriging (ORK) showed a relatively similar pattern to map obtained by IDW. However, the ORK map was smooth, presenting fewer duck-egg shapes (Fig. 5). The annual mean rainfall varied from 862 mm at the lowest elevation to 1334 mm at the highest elevation, with an areal mean of 1046 mm.

The trend modelled as a polynomial function of geographical coordinates was used to enhance the estimation by Universal Kriging (UNK) method. The influence of coordinates could make the map smoother than the map obtained by ORK (Fig. 5). However, the average areal rainfall was 1052 mm, a bit higher than the value obtained using previous methods. The annual mean rainfall varied from 851 mm at the lowest elevation to 1340 mm at the highest elevation.

We also integrated the elevation information extracted from Digital Elevation Model (DEM) in order to improve the previous estimation by using the Kriging with an External Drift (KED). The latter used the elevations as the secondary variable to derive the local mean of rainfall (primary variable). A visible high influence of topography over the estimated precipitation values appears clearly in the map (Fig. 5). Overall, KED tended to overestimate the annual mean rainfall over the area (1065 mm). The annual mean rainfall varied from 848 mm at the lowest elevation to 1406 mm at the highest elevation.

A multivariate extension of kriging, Ordinary Cokriging (OCK), was also used by

## Spatial interpolation of daily rainfall

S. Ly et al.

Title Page

Abstract

Introduction

Conclusions

References

Tables

Figures

◀

▶

◀

▶

Back

Close

Full Screen / Esc

Printer-friendly Version

Interactive Discussion



incorporating the elevation derived from DEM as secondary information. The elevation was known in each grid and varied smoothly across the study area (Fig. 3). The map derived using the OCK technique was very similar to those derived using the UNK and ORK methods (Fig. 5). Moreover, the mean rainfall over the area was also in the same range as the mean of THI, IDW, ORK and UNK methods. The annual mean rainfall varied from 847 mm at the lowest elevation to 1327 mm at the highest elevation with mean over area of 1050 mm.

However, when the fewest gages were used for interpolation, UNK and KED provided very poor results (Fig. 6) and over-estimated the annual mean rainfall. The annual mean rainfall generated by UNK and KED varied from 558 mm and 298 mm at the lowest elevation to 2391 mm and 3719 mm at the highest elevation, with a mean of 1141 mm and 1214 mm, respectively. This was due to the extrapolation of the UNK and KED outside the range of data. The values of the local trend (coordinate function) and sampled secondary variable (elevation) were outside the range of the values at locations where the primary variable were also sampled.

### 3.2 Performance of daily rainfall interpolators

The Rotbertville raingage with a high elevation (514.82 m) and situated near to the catchment's border always provided the highest RMSE value in all of the gage-degenerated cases (Fig. 7). However, Tailles, a raingage with the highest elevation (608.67 m) and situated in the peak line between the two catchments provided the second highest RMSE value.

The number of gages was the key factor for gradually reducing the RMSE (Fig. 8). There were little differences between geostatistical and IDW methods. However, the RMSE of estimates made using Thiessen polygon was clearly higher than those resulting from using geostatistics and IDW. When the number of gages becomes very small, the RMSE becomes very high and the difference in the RMSE between the methods becomes larger.

Geostatistical methods tended to increase the RMSE values, while IDW always

## Spatial interpolation of daily rainfall

S. Ly et al.

Title Page

Abstract

Introduction

Conclusions

References

Tables

Figures



Back

Close

Full Screen / Esc

Printer-friendly Version

Interactive Discussion



tended to decrease these values gradually when using all the raingages. Geostatistics and IDW considerably outperformed the Thiessen polygon method. The Thiessen polygon provided the largest average RMSE value (2.81 mm), while ORK gave the lowest average RMSE value (2.42 mm). Other methods gave a somewhat higher average RMSE than ORK-IDW (2.44 mm), UNK (2.49 mm), KED (2.50 mm) and OCK (2.53 mm). But their RMSE values stayed much lower than those of the Thiessen Polygon.

There was a sudden decline in Thiessen-polygon RMSE value when using eight raingages for interpolation (Fig. 8) because the eight raingages are close to the seven raingages selected for validation. Although, RMSE values, provided by geostatistical and IDW methods, gradually decreased according to the number of raingages used for the interpolation (Fig. 8). In general, the values of points close to the sample points are more likely to be similar than those that are further apart. The Thiessen polygon ignored the pattern of spatial dependence and considered only one measurement, whereas IDW and geostatistics were respectively based on the surrounding measured values and statistical models that included autocorrelation – the statistical relationship between the measured points.

For ORK, estimates based on more raingages tended to produce lower RMSE values. ORK outperformed the technique in most cases, while IDW provided lowest RMSE values where 8 and 20 gages were used. UNK provided the second lowest RMSE values where 50 and 60 raingages were used.

## 4 Discussion

Results from the application of different algorithms provided some insights in terms of strengths and weaknesses, and in term of the applicability of the deterministic and geostatistical methods to daily rainfall made using different densities of raingages in the Ourthe and Ambleve catchments. All the algorithms were able to produce 30-year daily rainfall on the catchment grids for a distributed hydrological model, ranging from

## Spatial interpolation of daily rainfall

S. Ly et al.

Title Page

Abstract

Introduction

Conclusions

References

Tables

Figures



Back

Close

Full Screen / Esc

Printer-friendly Version

Interactive Discussion



the most straightforward (THI) to the most complex method (OCK). This process is very important because there is little evidence that any one method is optimal across a range of conditions.

The geostatistical and IDW methods outperform the Thiessen polygon method for the Ourthe and Ambleve catchments. However, this study suggests that gage density was one of the major factors in determining the performance of such interpolation method (Fig. 8). Here, the best methods are ORK and IDW for daily rainfall. This is consistent with the finding of cross validation from the interpolation of average daily rainfall in the South Ecuadorian Paramo conducted by Buytaert et al. (2006) and daily rainfall interpolation on a large scale basin in West Africa validated by hydrological modelling (Ruelland et al., 2008).

The present study also shows that IDW had a smaller error of estimates than ORK and UNK when using 30, 20, 8 and 4 gages (Fig. 8). IDW weight is the inverse distance of the neighbour points while kriging weight is determined by semi-variogram that made using spatial relationship of both distances and values of the neighbour points. So the IDW is the most adequate because the stations used for interpolation of these cases may be close to the seven stations for validation. This finding is consistent with the conclusions of Nalder and Wein (1998) – IDW has a smaller error of estimates than ORK and UNK in interpolating monthly precipitation in the Canadian boreal forest. This result also confirmed previous findings by Dirks et al. (1998), who recommended the use of IDW for interpolation. But, they worked on the spatially dense networks in Norfolk Island.

When using 50 and 60 raingages, UNK produced RMSE values lower than IDW (Fig. 8). This is comparable to the conclusions of Basistha et al. (2008), who reported that UNK was the most suitable method, followed by ORK and IDW. The study of Basistha et al. (2008) involved the interpolation of annual rainfall in the Himalayas where the elevation lies from 175 m to 7409 m with 44 stations over an area of 53 484 km<sup>2</sup>.

However, UNK and KED showed some limitations and tended to over-estimate the mean rainfall over the catchment area. In particular, the most critical case in this study

## Spatial interpolation of daily rainfall

S. Ly et al.

Title Page

Abstract

Introduction

Conclusions

References

Tables

Figures

◀

▶

◀

▶

Back

Close

Full Screen / Esc

Printer-friendly Version

Interactive Discussion



used the fewest raingages, which were only at the low-elevation part of the catchment area. UNK and KED produced very poor results in term of both rainfall distribution and accuracy at raingages used for validation. The rainfall distributions were very poorly represented. The RMSE values were very high.

Integrating elevation into KED and OCK for spatial interpolation did not really lead to a smaller error of estimates here and showed the highest RMSE value between IDW and other geostatistical methods for most of the gage-degenerated cases (Fig. 8). This is because of the poor correlation between elevation and daily rainfall (Fig. 4). Certainly, differences in the time step used for interpolation could contribute to the difference in the result of the present study and those of studies of Goovaert (2000) and Lloyd (2005), which used monthly and annual time steps. Accounting for elevation using multivariate geostatistical algorithms (KED and OCK) generally reduces the ORK prediction error as long as the correlation coefficient is larger than 0.75. The benefit of multivariate techniques can, therefore, become marginal if the correlation between rainfall and elevation is too small (Goovaert, 2000). When the observation time steps are less than one a month, the location relationship between precipitation and altitude is likely to be less obvious (Lloyd, 2005). In his study, the rainfall accumulations were measured in shorter time steps (daily) and the correlation was relatively small for most of the rain days (Fig. 4). Hence, ORK and IDW provided better results than the other methods.

## 5 Conclusions

Our results confirm that for daily rainfall, geostatistical and IDW algorithms significantly outperform simple techniques like the Thiessen polygon which is commonly used in various hydrological models. Here, the Thiessen polygon clearly provided a discontinuous rain field at the border of each polygon, and did not show the true spatial variation of rainfall. Average RMSE values from the validated gages were always highest in all gage-degenerated cases.

### Spatial interpolation of daily rainfall

S. Ly et al.

Title Page

Abstract

Introduction

Conclusions

References

Tables

Figures



Back

Close

Full Screen / Esc

Printer-friendly Version

Interactive Discussion



## Spatial interpolation of daily rainfall

S. Ly et al.

Title Page

Abstract

Introduction

Conclusions

References

Tables

Figures

◀

▶

◀

▶

Back

Close

Full Screen / Esc

Printer-friendly Version

Interactive Discussion



We recommended that care should be taken in using UNK and KED when interpolating with very few neighbourhood sample points. These methods can extrapolate outside the range of data values and cause a poor result. Between the geostatistical and IDW methods, KED and OCK are not supposed to be the improved methods because the correlation of daily rainfall and elevation was small for most of the rain days.

ORK was considered to be the best method since it provided lowest RMSE value for nearly all cases. This method was followed by IDW. However, the IDW method was much simpler than complex geostatistical methods which require a lot of time for computation.

However, we dealt only with data at seven raingages in order to assess the performance of the different methods. Further research should combine cross validation with all time series of existing data for a fuller assessment of the strengths and weaknesses of the approaches used. A subject that remains to be explored is what methods that produce daily rainfall for a distributed hydrological model can provide the best results for stream flow simulation.

*Acknowledgement.* This study was financially supported by the scholarship programme of the cooperation project CUI-ITC01 funded by CUD (Coopération Universitaire pour le Développement) of Belgium. Rainfall data were given free of charge by SETHY (le Service public de Wallonie, Direction générale opérationnelle Mobilité et Voies hydrauliques, Direction de la Gestion hydrologique intégrée, Service d'Etude Hydrologique) and ERRUISSOL (EROSion RUIssellement Sol).

## References

- Andréassian, V., Perrain, C., Michel, C., Usart-Sanchez, I., and Lavabre, J.: Impact of imperfect rainfall knowledge on efficiency and the parameters of watershed models, *J. Hydrol.*, 250, 206–223, 2001.
- Angulo-Martínez, M. López-Vicente, S., Vicente-Serrano, S. M., and Beguería, S.: Mapping rainfall erosivity at a regional scale: a comparison of interpolation methods in the Ebro

## Spatial interpolation of daily rainfall

S. Ly et al.

[Title Page](#)
[Abstract](#)
[Introduction](#)
[Conclusions](#)
[References](#)
[Tables](#)
[Figures](#)
[◀](#)
[▶](#)
[◀](#)
[▶](#)
[Back](#)
[Close](#)
[Full Screen / Esc](#)
[Printer-friendly Version](#)
[Interactive Discussion](#)


Basin (NE Spain), *Hydrol. Earth Syst. Sci.*, 13, 1907–1920, doi:10.5194/hess-13-1907-2009, 2009a.

Angulo-Martínez, M. and Beguería, S.: Estimating rainfall erosivity from daily precipitation records: A comparison among methods using data from the Ebro Basin (NE Spain), *J. Hydrol.*, 379, 111–121, 2009b.

Aronica, G. and Ferro, V.: Rainfall erosivity over the Calabrian region/Erosivité des précipitations en Calabre', *Hydrol. Sci. J.*, 42(1), 35–48, 1997.

Attorre, F., Alfo, M., Sanctis, M. D., Francesconi, F., and Bruno, F.: Comparison of interpolation methods for mapping climatic and bioclimatic variables at regional scale, *Int. J. Climatol.*, 27, 1825–1843, 2007.

Basistha, A., Arya, D. S., and Goel, N. K.: Spatial distribution of rainfall in Indian Himalayas – a case study of Uttarakhand region, *Water Resour. Manag.*, 22, 1325–1346, 2008.

Boer, E. P. J., de Beurs, K. M., and Hartkamp, A. D.: Kriging and thin plate splines for mapping climate variables, *Int. J. Appl. Earth Obs. Geoinf.*, 3(2), 146–154, 2001.

Buytaert, W., Celleri, R., Willems, P., Bièvre, D. B., and Wyseure, G.: Spatial and temporal rainfall variability in mountainous areas: a case study from the South Ecuadorian Andes, *J. Hydrol.*, 329, 413–421, 2006.

Caruso, C. and Quarta, F.: Interpolation methods comparison, *Comput. Math. Appl.*, 35(12), 109–126, 1998.

Chaubey, I., Haan, C. T., Grunwald, S., and Salisbury, J. M.: Uncertainty in the model parameters due to spatial variability of rainfall, *J. Hydrol.* 220, 48–61, 1999.

Chilès, J. P. and Delfiner, P.: *Geostatistics: Modelling Spatial Uncertainty*, John Wiley & Sons, New York, 1999.

Chow, V. T.: *Handbook of Applied Hydrology: a Compendium of Water-Resources Technology*, McGraw-Hill, Inc. 1964.

Cole, S. J. and Moore, R. J.: Hydrological modelling using raingage and radar-based estimators of areal rainfall, *J. Hydrol.*, 358, 159–181, 2008.

Collischonn, B., Collischonn, W., and Tucci, C. E. M.: Daily hydrological modeling in the Amazon basin using TRMM rainfall estimates, *J. Hydrol.*, 360, 207–216, 2008.

Cressie, N.: Fitting variogram models by weighted least squares, *Math. Geol.*, 17, 563–586, 1985.

Cressie, N.: *Statistics for Spatial Data*, Wiley, New York, 900 pp., 1991.

Demarcin, P., Degre, A., Smoos, A., and Dautrebande, S.: *Projet ERRUISSOL. Cartographie*

## Spatial interpolation of daily rainfall

S. Ly et al.

Title Page

Abstract

Introduction

Conclusions

References

Tables

Figures

◀

▶

◀

▶

Back

Close

Full Screen / Esc

Printer-friendly Version

Interactive Discussion



numérique des zones à risque de ruissellement et d'érosion des sols en Région wallonne (Belgique). Rapport final de convention DGO3, Unité d'hydrologie et hydraulique agricole, Faculté Universitaire des Sciences Agronomiques de Gembloux, 55 pp., 2009.

Dirks, K. N., Hay, J. E., Stow, C. D., and Harris, D.: High-resolution of rainfall on Norfolk Island, Part II: Interpolation of rainfall data, *J. Hydrol.*, 208, 187–193, 1998.

Faurès, J. M., Goodrich, D. C., Woolhiser, D. A., and Sorooshian, S.: Impact of small-scale spatial variability on runoff modeling, *J. Hydrol.*, 173, 309–326, 1995.

Gabellani, S., Boni, G., Ferraris, L., Hardenberg, J. V., and Provenzale, A.: Propagation of uncertainty from rainfall to runoff: a case study with a stochastic rainfall generator, *Adv. Water Resour.*, 30, 2061–2071, 2007.

Goovaerts, P.: *Geostatistics for Natural Resources Evaluation*, Oxford University Press, New York, 483 pp., 1997.

Goovaerts, P.: Geostatistical tools for characterizing the spatial variability of microbiological and physico-chemical soil properties, *Biol. Fert. Soils.*, 27, 315–334, 1998.

Goovaerts, P.: Using elevation to aid the geostatistical mapping of rainfall erosivity, *Catena*, 34, 227–242, 1999.

Goovaerts, P.: Geostatistical approaches for incorporating elevation into the spatial interpolation of rainfall, *J. Hydrol.*, 228, 113–129, 2000.

Haberlandt, U.: Geostatistical interpolation of hourly precipitation from rain gauges and radar for a large-scale extreme rainfall event, *J. Hydrol.*, 332, 144–157, 2007.

Hevesi, J., Istok, J., and Flint, A.: Precipitation estimation in mountainous terrain using multivariate geostatistics. Part I: structural analysis, *J. Appl. Meteorol.*, 31, 661–676, 1992.

Hoyos, N., Waylena, P. R., and Jaramillo, A.: Seasonal and spatial patterns of erosivity in a tropical watershed of the Colombian Andes, *J. Hydrol.*, 314, 177–191, 2005.

Isaaks, E. H. and Srivastava, R. M.: *An Introduction to Applied Geostatistics*. Oxford University Press, New York, 561 pp., 1989.

Kobold, M. and Sušelj, K.: Precipitation forecasts and their uncertainty as input into hydrological models, *Hydrol. Earth Syst. Sci.*, 9, 322–332, doi:10.5194/hess-9-322-2005, 2005.

Lanza, L. G., Ramírez, J. A., and Todini, E.: Stochastic rainfall interpolation and downscaling, *Hydrol. Earth Syst. Sci.*, 5, 139–143, doi:10.5194/hess-5-139-2001, 2001.

Leander, R., Buishand, T. A., van den Hurk, B. J. J. M., and de Wit, M. J. M.: Estimated changes in flood quantiles of the river Meuse from resampling of regional climate model output, *J. Hydrol.*, 351, 331–343, 2008.

## Spatial interpolation of daily rainfall

S. Ly et al.

[Title Page](#)
[Abstract](#)
[Introduction](#)
[Conclusions](#)
[References](#)
[Tables](#)
[Figures](#)
[◀](#)
[▶](#)
[◀](#)
[▶](#)
[Back](#)
[Close](#)
[Full Screen / Esc](#)
[Printer-friendly Version](#)
[Interactive Discussion](#)


- Lloyd, C. D.: Assessing the effect of integrating elevation data into the estimation of monthly precipitation in Great Britain, *J. Hydrol.*, 308, 128–150, 2005.
- Lu, G. Y. and Wong, D. W.: An adaptive inverse-distance weighting spatial interpolation technique, *Comput. Geosci.*, 34, 1044–1055, 2008.
- 5 Matheron, G.: *The Theory of Regionalised Variables and its Applications: Les Cahiers du Centre de Morphologie Mathématique de Fontainebleau No. 5*, The Ecole Nationale Supérieure des Mines de Paris, Paris, France, 1971.
- Marquínez, J., Lastra, J., and García, P.: Estimation models for precipitation in mountainous regions: the use of GIS and multivariate analysis, *J. Hydrol.*, 270, 1–11, 2003.
- 10 Moulin, L., Gaume, E., and Obled, C.: Uncertainties on mean areal precipitation: assessment and impact on streamflow simulations, *Hydrol. Earth Syst. Sci.*, 13, 99–114, doi:10.5194/hess-13-99-2009, 2009.
- Nalder, I. A. and Wein, R. W.: Spatial interpolation of climatic normals: test of a new method in the Canadian boreal forest, *Agr. Forest Meteorol.*, 92, 211–225, 1998.
- 15 Nyssen, J., Vandenreyken, H., Poesen, J., Moeyersons, J., and Deckers, J.: Rainfall erosivity and variability in the Northern Ethiopian Highlands, *J. Hydrol.*, 311, 172–187, 2005.
- Ruelland, D., Ardoin-Bardin, S., Billen, G., and Servat, E.: Sensitivity of a lumped and semi-distributed hydrological model to several methods of rainfall interpolation on a large basin in West Africa, *J. Hydrol.*, 361, 96–117, 2008.
- 20 Schuurmans, J. M. and Bierkens, M. F. P.: Effect of spatial distribution of daily rainfall on interior catchment response of a distributed hydrological model, *Hydrol. Earth Syst. Sci.*, 11, 677–693, doi:10.5194/hess-11-677-2007, 2007.
- Singh, V. P.: Effect of spatial and temporal variability in rainfall and watershed characteristics on stream flow hydrograph, *Hydrol. Process.*, 11(11), 1649–1669, 1997.
- 25 Syed, K. H., Goodrich, D. C., Myers, D. E., and Sorooshian, S.: Spatial characteristics of thunderstorm rainfall fields and their relation to runoff, *J. Hydrol.*, 271, 1–21, 2003.
- Teegavarapu, R. and Chandramouli, V.: Improved weighting methods, deterministic and stochastic data-driven models for estimation of missing precipitation records, *J. Hydrol.*, 312, 191–206, 2005.
- 30 Todini, E., Pellegrini, F., and Mazzetti, C.: Influence of parameter estimation uncertainty in Kriging: Part 2 – Test and case study applications, *Hydrol. Earth Syst. Sci.*, 5, 225–232, doi:10.5194/hess-5-225-2001, 2001.

Vicent-Serrano, S. M., Saz-Sanchez, M. A., and Cuadrat, J. M.: Comparative analysis of interpolation methods in the middle Ebro Valley (Spain): application to annual precipitation and temperature, *Climate Res.*, 24, 161–180, 2003.

Webster, R. and Oliver, M. A.: *Geostatistics for Environmental Scientists*, Statistics in Practice Series, John Wiley & Son Ltd., 315 pp., 2007.

5

## Spatial interpolation of daily rainfall

S. Ly et al.

Title Page

Abstract

Introduction

Conclusions

References

Tables

Figures



Back

Close

Full Screen / Esc

Printer-friendly Version

Interactive Discussion



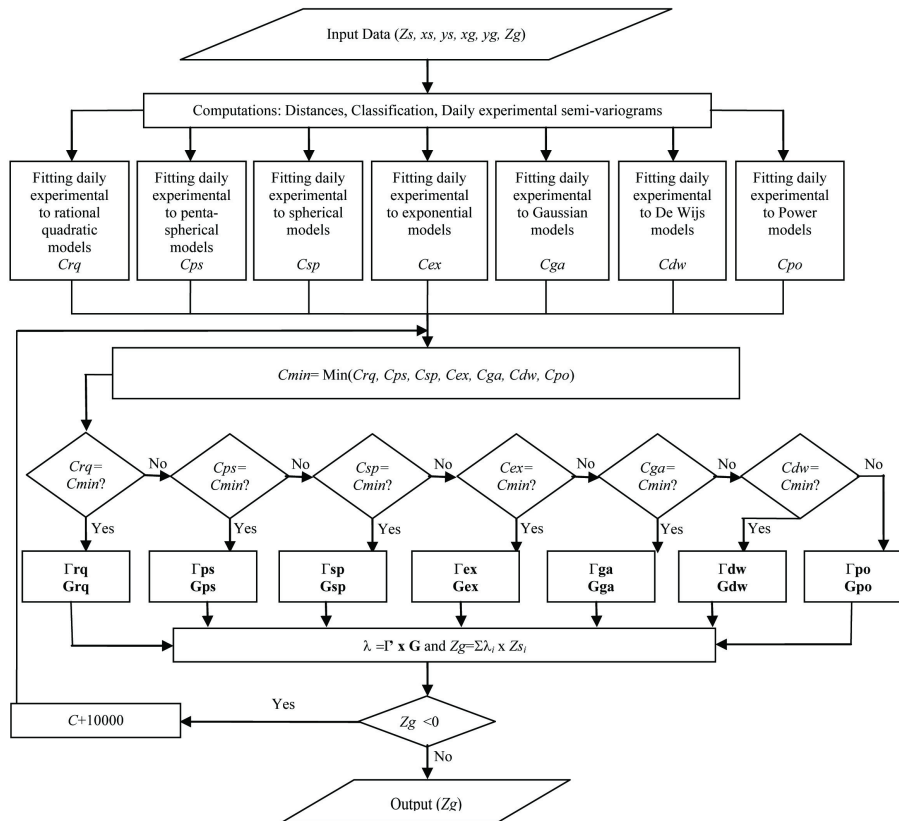


Fig. 1. Flowchart showing the simplified procedure of kriging computation.

Title Page

Abstract

Introduction

Conclusions

References

Tables

Figures

◀

▶

◀

▶

Back

Close

Full Screen / Esc

Printer-friendly Version

Interactive Discussion



## Spatial interpolation of daily rainfall

S. Ly et al.

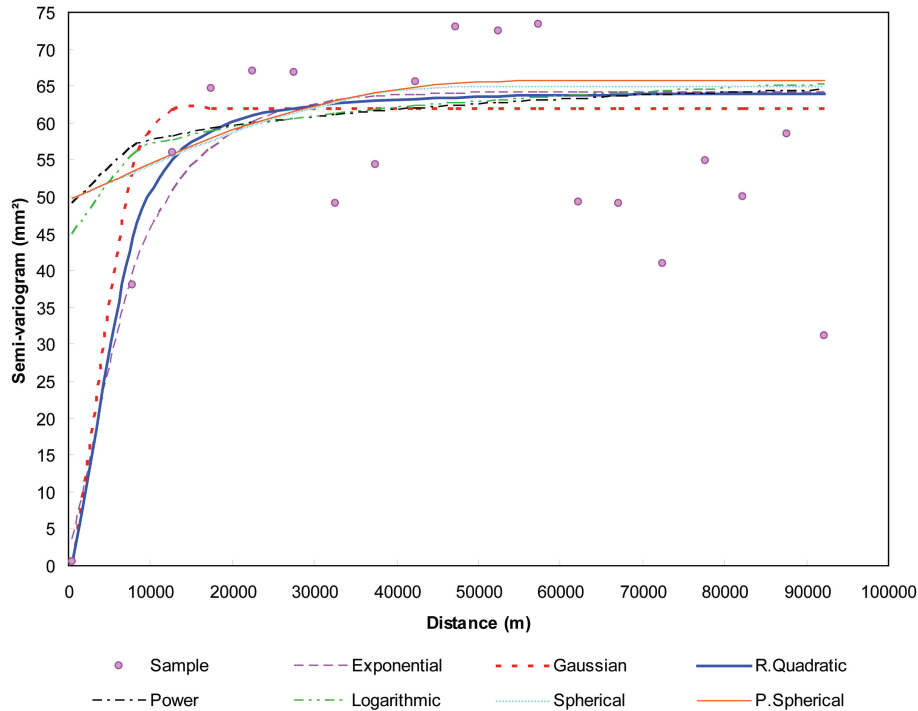


**Fig. 2.** Sample semivariogram of daily rainfall (7 August 1991) with seven models fitted: the Rational Quadratic Model is best fitted.

[Title Page](#)  
[Abstract](#)   [Introduction](#)  
[Conclusions](#)   [References](#)  
[Tables](#)   [Figures](#)  
[◀](#)   [▶](#)  
[◀](#)   [▶](#)  
[Back](#)   [Close](#)  
[Full Screen / Esc](#)  
[Printer-friendly Version](#)  
[Interactive Discussion](#)



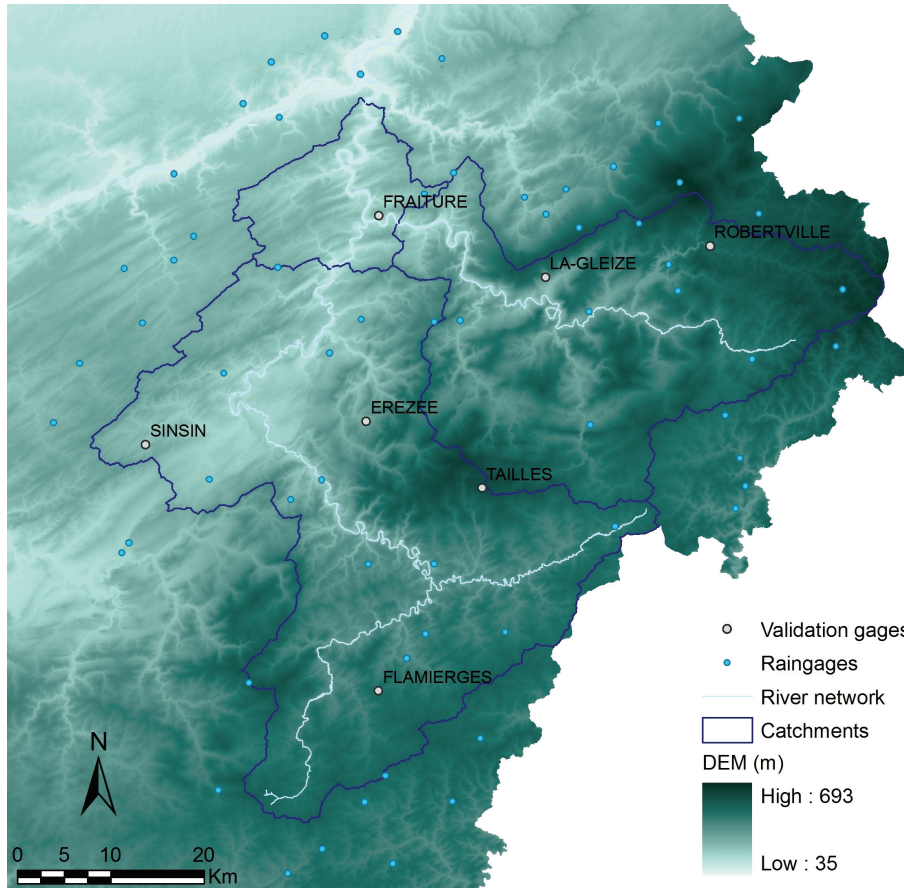


**Fig. 3.** Location of raingages and Digital Elevation Model of the Ourthe and Ambleve catchments, Walloon, Belgium.

## Spatial interpolation of daily rainfall

S. Ly et al.

<a href="#">Title Page</a>	
<a href="#">Abstract</a>	<a href="#">Introduction</a>
<a href="#">Conclusions</a>	<a href="#">References</a>
<a href="#">Tables</a>	<a href="#">Figures</a>
<a href="#">◀</a>	<a href="#">▶</a>
<a href="#">◀</a>	<a href="#">▶</a>
<a href="#">Back</a>	<a href="#">Close</a>
<a href="#">Full Screen / Esc</a>	
<a href="#">Printer-friendly Version</a>	
<a href="#">Interactive Discussion</a>	



## Spatial interpolation of daily rainfall

S. Ly et al.

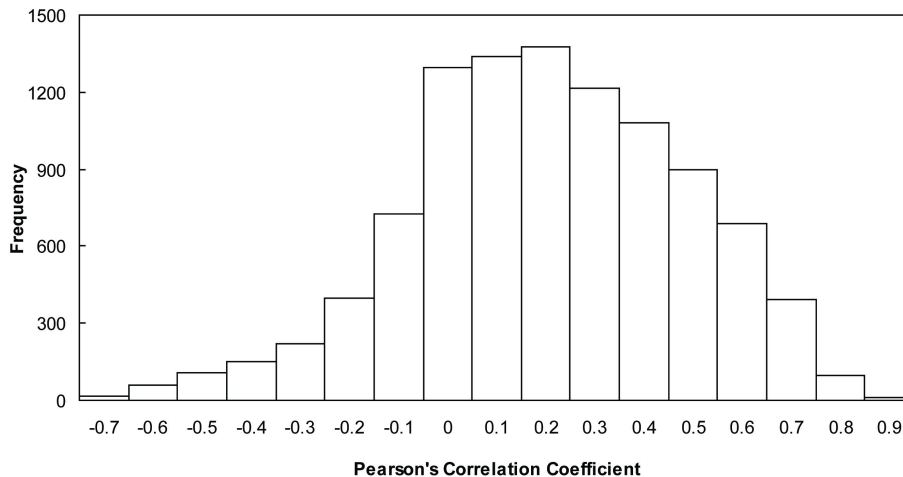


**Fig. 4.** Histogram of Pearson's correlation coefficient of daily rainfall (1976–2005) and altitude extracted from DEM.

Title Page

Abstract	Introduction
Conclusions	References
Tables	Figures

⏪
⏩

◀
▶

Back
Close

Full Screen / Esc

Printer-friendly Version

Interactive Discussion



## Spatial interpolation of daily rainfall

S. Ly et al.

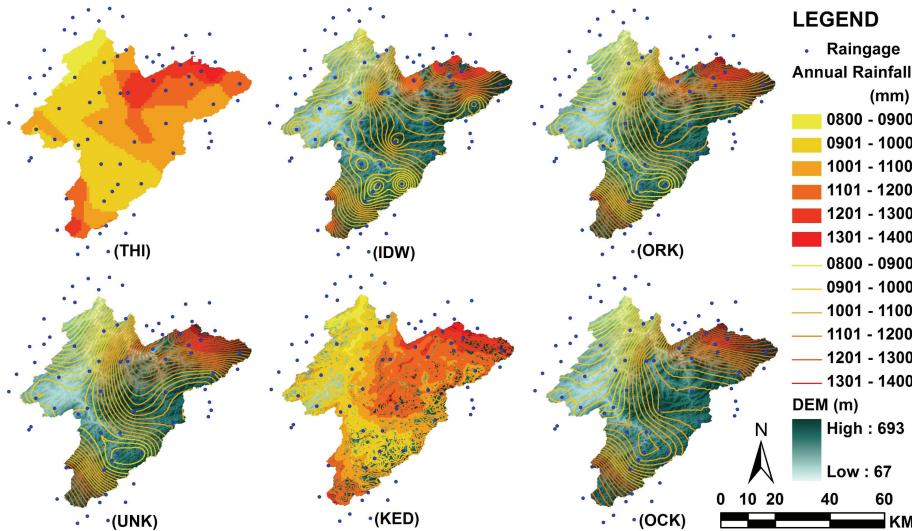


**Fig. 5.** Annual mean rainfall of the Ourthe and Ambleve catchments, generated using six different algorithms and 70 raingages available in and surrounding the two catchments: 10-mm intervals of hysoyetal contours.

Title Page

Abstract Introduction

Conclusions References

Tables Figures

◀ ▶

◀ ▶

Back Close

Full Screen / Esc

Printer-friendly Version

Interactive Discussion





## Spatial interpolation of daily rainfall

S. Ly et al.

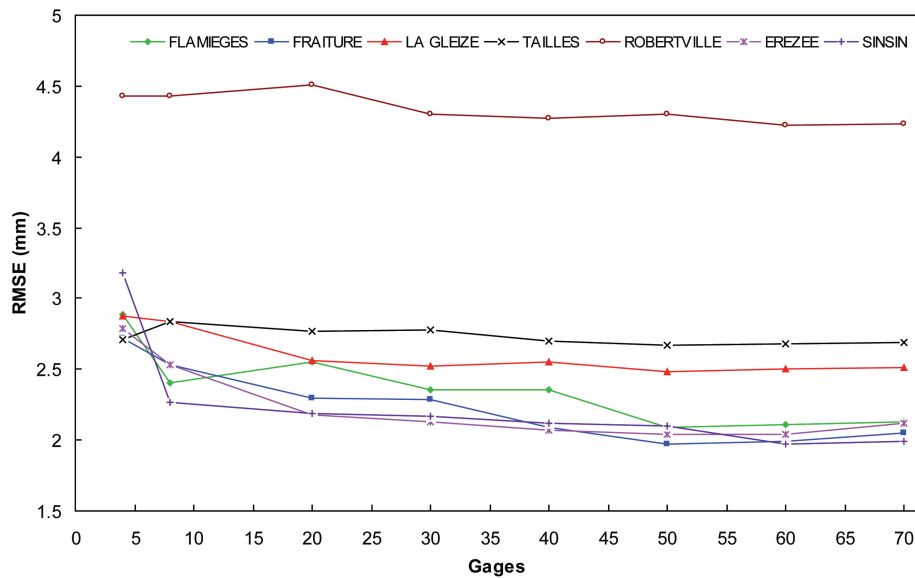


**Fig. 7.** Evolution of average RMSE values of different validation gages according to number of gages used for interpolation.

Title Page

Abstract Introduction

Conclusions References

Tables Figures

◀ ▶

◀ ▶

Back Close

Full Screen / Esc

Printer-friendly Version

Interactive Discussion



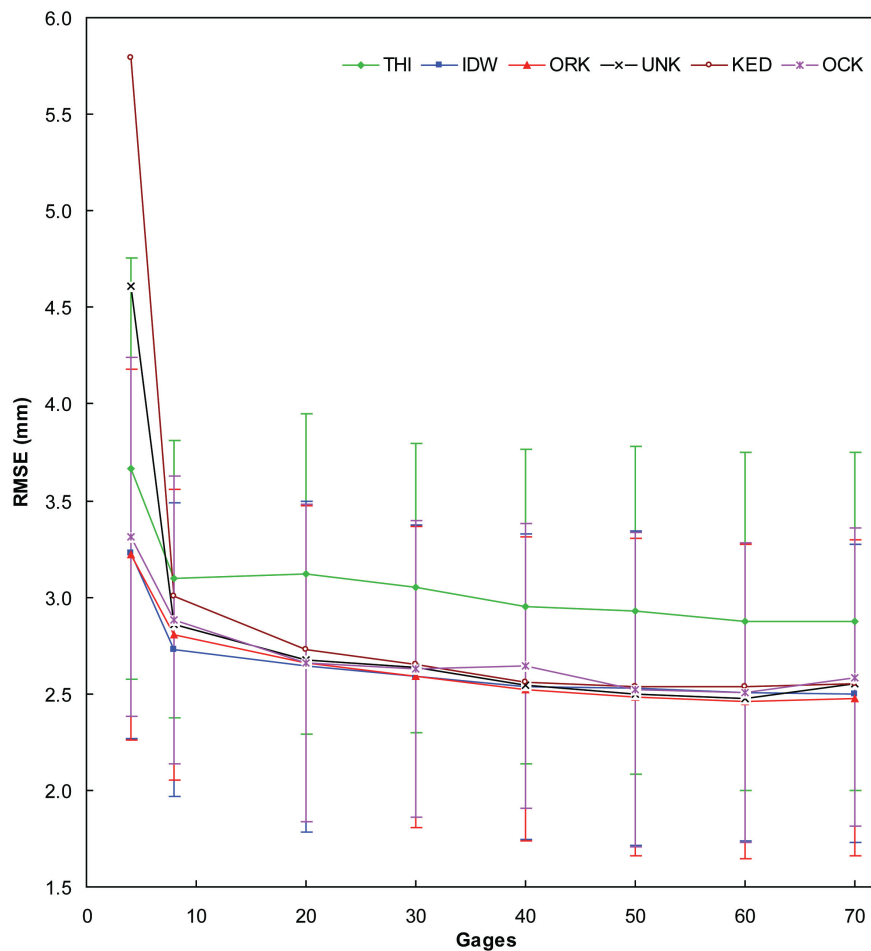


Fig. 8. Evolution of RMSE values of different methods according to number of gages.

## Spatial interpolation of daily rainfall

S. Ly et al.

Title Page

Abstract Introduction

Conclusions References

Tables Figures

◀ ▶

◀ ▶

Back Close

Full Screen / Esc

Printer-friendly Version

Interactive Discussion

